

Spatial correlations in the relaxation of the Kob-Andersen model

ENZO MARINARI¹ AND ESTELLE PITARD²

¹ *Dipartimento di Fisica, SMC and UdR1 of INFN, INFN, Università di Roma La Sapienza, P.le Aldo Moro 2, 00185 Roma, Italy.*

² *Laboratoire des Verres (CNRS-UMR n°5587), CC69, Université Montpellier 2, 34095 Montpellier Cedex 5, France.*

PACS. 64.70.Pf – Glass transitions.

PACS. 05.50.+q – Lattice theory and statistics.

PACS. 61.20.Lc – Time-dependent properties of liquid structure; relaxation.

Abstract. – We describe spatio-temporal correlations and heterogeneities in a kinetically constrained glassy model, the Kob-Andersen model. The kinetic constraints of the model alone induce the existence of dynamic correlation lengths, that increase as the density ρ increases, in a way compatible with a double-exponential law. We characterize in detail the trapping time correlation length, the cooperativity length, and the distribution of persistent clusters of particles. This last quantity is related to the typical size of blocked clusters that slow down the dynamics for a given density.

Glassy dynamics in kinetically constrained systems has been a subject of wide interest during the last years [1]. It indeed includes a large class of models of particles constrained by dynamical rules where the relaxation is slowed down when the density of particles increases or the temperature decreases, sharing similarities (though with a number of differences) with spin-glass models or glass models [2] when the temperature is decreased. In the former class, slowing down of the dynamics can be understood as a consequence of steric effects, that make certain moves of particles impossible because of an effective high local density, putting strong constraints on the number of allowed paths between configurations [3]; whereas for the latter class, frustration and/or disorder in the interactions produces a slow time relaxation. In real glasses both effects are likely to be present. While most studies on the glass state have focused for a long time on the latter class of models, more attention is paid to the fact that the former mechanism is also of importance, especially since the works of Harrowell [4] on spatio-temporal heterogeneities. These heterogeneities are also of great interest for experimentalists, since they have been identified in several glassy systems [5].

In this paper we will focus on the numerical study of the Kob-Andersen (KA) model [6]. In this 3-dimensional model of lattice gas on a cubic lattice, a particle can hop to one of its empty nearest neighbor sites only if it has strictly less than m occupied nearest-neighbor sites, and if after the hop it will also have less than m occupied nearest-neighbor sites (which ensures detailed balance). In the original study of the KA model, the value of m is chosen

to be $m = 4$, which is a compromise between free diffusion of particles with excluded volume ($m = 6$) and a truly non-ergodic model (for $m \leq 3$ small cubes of occupied sites are blocked for ever). The relaxation is hence a diffusive process with additional steric constraints. The energy landscape is trivial in the sense that there is no interaction between particles, hence all configurations are thermodynamically equally probable. However the original numerical study of the KA model showed features similar to those seen in glassy systems such as the arrest of the diffusion constant at some density ρ_c smaller than 1 ($\rho_c \simeq 0.881$ in [6]), and slow stretched-exponential relaxation of the intermediate scattering function; though, it was already pointed out by the authors that the Mode-Coupling predictions for glasses are actually not valid for this model. Moreover, the dynamics is time translationally invariant (there is no aging), because all configurations are equivalent. One way to induce aging is to do density crunches (i.e quenches to higher densities) in a system where a reservoir of particles is added, as studied in [7], or to add explicit two-body interactions between the particles.

Recently the question of finite-size effects in the KA model, already addressed in [6], came back, related to the still unsolved issue of a true dynamical transition in the thermodynamic limit. It is now established that in the thermodynamic limit and in finite dimension, no dynamical arrest occurs at a density smaller than one [9–11]; whereas in a mean-field version of the model on a Bethe lattice, such a dynamical transition at $\rho_c < 1$ occurs. More precisely, the critical density in three dimensions depends on the size L of the system like $1 - \rho_c(L) = C/(\ln(\ln L))$, where C is a constant, which makes the convergence to 1 very slow and unreachable by numerical simulations. In other words, at fixed density ρ , in order to eliminate finite size effects, one has to study system sizes much larger than the spacing between mobile particles $\Xi(\rho) \propto \exp(C/(1 - \rho))$.

Finally the KA model has been shown to share an important feature with the dynamics of mean-field spin-glass models and supercooled liquids [5, 12–15]: the dynamical susceptibility $\chi(t)$ shows a pronounced maximum at an intermediate time t^* , this maximum is interpreted as the time where heterogeneities are the strongest in the system, and increases as the density increases (analog to a decrease of temperature in other models), hinting at the existence of a growing correlation length. Because of its purely constrained nature (no energy barriers, no dynamical transition) the origin of these spatio-temporal heterogeneities in the KA model comes merely from steric effects [9, 16].

In this study we give a description of the spatio-temporal correlations and heterogeneities that characterize the dynamics of the KA model. First, we characterize the distribution of trapping times of particles (for recent work on different systems see for example [17, 18]) and its spatial correlations. Then we describe the behavior of the four-point spatio-temporal correlation functions in real space, giving a determination of a cooperative length-scale not provided a priori by $\chi(t)$, in an approach complementary to [19]. Finally we study the dynamics of the KA model in terms of the distribution of persistent clusters (this is a new approach to the problem), and show how spatial heterogeneity and cooperativity can be identified in this way. We show that the different lengths identified in this study behave in the way predicted by Toninelli, Biroli and Fisher [9–11] as a function of the density.

Trapping times. – We have computed the distribution of trapping times (or persistence times) $P(\tau)$. Let τ_i be the time after which the particle starting from site i first moves to one of its nearest-neighbor site: we calculate the probability for τ_i to have the value τ , and we average over all particles and over a large number of initial configurations of the system. We have computed $P(\tau)$ for different densities (ranging from 0.5 to 0.8, see figure 1). Our fits are consistent with a stretched exponential behavior for the integrated probability distribution, $\int_{\tau}^{\infty} dt P(t) = \exp\{-(\tau/\tau_{trap})^{\beta}\}$, where β decreases as the density increases

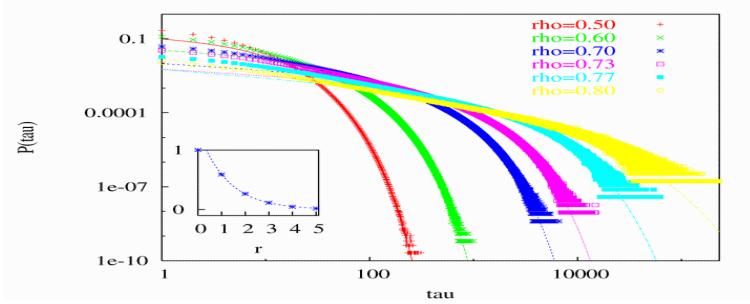


Fig. 1 – $P(\tau)$ versus τ in for different values of ρ . The smooth curves are for the stretched exponential best fits for the integrated probability. In the inset $C_\rho(r)$ for $\rho = 0.77$.

from 0.80 ($\rho = 0.5$) to 0.45 ($\rho = 0.8$). Such stretched exponential behavior also characterizes $P(\tau)$ in KCM, in Lennard-Jones systems and in experiments (see [8] and references therein). In particular, in the East model, a temperature dependent stretching exponent for $P(\tau)$ is observed [20].

The site dependent trapping times defined above do not need to be homogeneous in space. One can ask whether the KA dynamics induces a spatial correlation length among them. We have quantified this aspect by computing spatial correlations: $C_\rho(r) \equiv \frac{1}{N} \sum_{\vec{a}} (\langle \tau_{\vec{a}} \tau_{\vec{a}+\vec{r}} \rangle - \langle \tau_{\vec{a}} \rangle \langle \tau_{\vec{a}+\vec{r}} \rangle)$, where $\langle \dots \rangle$ stands for an average over initial configurations. $l_c(\rho)$ is a *dynamical coherence length* such that for distances larger than $l_c(\rho)$ the trapping times are uncorrelated. An exponential fit, where $C_\rho(r) \sim e^{-r/l_c(\rho)}$, done for r going from 1 to 5 works well. Although in the density range 0.7-0.8 $l_c(\rho)$ is small and of the order of one or two lattice spacings, the growth of $l_c(\rho)$ for increasing ρ (from 0.7 to 0.77) can be fitted by a double-exponential law $l_c(\rho) \simeq 0.17 \exp(\exp(0.16/(1-\rho)))$.

The finding of this stretched exponential behavior leads to consider the relaxation of correlation functions. Ref. [21] has analyzed stretched exponential relaxations in glassy systems, looking at it as a consequence of a renewal process for a single effective particle, where the distribution of renewal times is itself a stretched exponential, leading to stretched-exponential relaxation with the same exponent for the time correlations. It is not obvious whether the cooperative dynamics of the KA model could be mapped onto such a simple renewal process with a distribution of times equal to the distribution of persistence times $P(\tau)$. To test this, we define the overlap function as $q(t) \equiv \frac{1}{N\rho(1-\rho)} \sum_i (n_i(t)n_i(0) - \rho^2)$, where $n_i(t) = 0$ or 1 is the occupation number of site i at time t . We have computed $\langle q(t) \rangle$ as an average over initial configurations. Even if in the asymptotic time regime $\langle q(t) \rangle$ should decay as a power law [22], we do not see any sign of this behavior ⁽¹⁾: it is in fact very well fitted by a stretched exponential, with a stretching exponent that depends on ρ , $\langle q(t) \rangle \sim \exp(-(t/t_{relax})^\gamma)$. γ decreases from 0.8 to 0.35 for ρ increasing from 0.5 to 0.8. The exact values of γ are not identical to the ones of β , but they are very similar: in the limits of the statistical and systematic error, that we estimate to be smaller than 0.05, we find the values compatible. A possible real discrepancy of the two exponents would be a signal of the fact that the growth of spatial correlations with density (although $l_c(\rho)$ is always small in our simulations) plays an important role, and that the KA model can not be reduced to a unique effective renewal process. Instead, one has to take into account the spatial correlations of the dynamics.

⁽¹⁾We have checked that even in the unconstrained lattice gas for high density values we are not able to observe a simple power law decay.

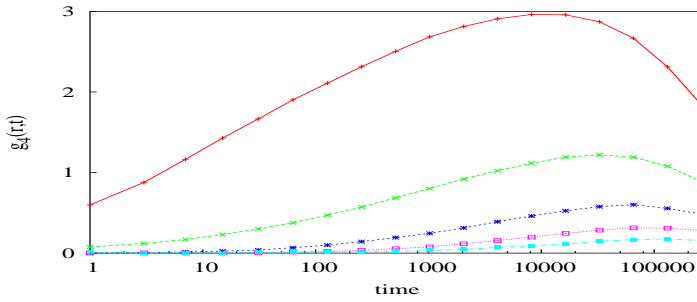


Fig. 2 – $g_4(r, t)$ for $\rho = 0.85$ and $L = 24$ as a function of time. From top to bottom, $r = 1, 2, 3, 4, 5$.

Spatio-temporal correlation functions. – The dynamic susceptibility $\chi(t) \equiv N (\langle q^2(t) \rangle - \langle q(t) \rangle^2)$ has been one of the main evidences presented in [15] stressing the relation of the KA model to liquids and spin glasses: as a function of time it shows a maximum at t^* , where the sensitivity of the system is maximal. We have repeated with larger precision, for a range of densities, the measurements of [15], finding compatible results. Both the value of the maximum of $\chi(t)$ and t^* as a function of ρ are very well fitted by the double-exponential scaling form of [10] (see also Figure 6). At $t = t^*$ (which is of the same order of magnitude as the relaxation time) the statistical heterogeneity of the system is maximal. We show now that it is also related to spatial cooperativity and heterogeneity.

We define and measure a space-dependent susceptibility $g_4(\vec{r}, t)$, which generalizes $\chi(t)$ [14]:

$$g_4(r, t) \equiv (N\rho^2(1-\rho)^2)^{-1} \sum_{|\vec{r}_i - \vec{r}_j|=r} (\langle n_i(t)n_i(0)n_j(t)n_j(0) \rangle - \langle n_i(t)n_i(0) \rangle \langle n_j(t)n_j(0) \rangle) . \quad (1)$$

Here we only take the spatial separation on a single coordinate axis, so that r is at the same time an Euclidean and a Manhattan distance. We show $g_4(\vec{r}, t)$ as a function of time in figure 2: for all values of r it shows a maximum. The position of the maximum is of the same order of magnitude as t^* but shifts to larger times as r increases. The value of the maximum is decreasing with r .

The function $g_4(\vec{r}, t)$ gives information on how the decorrelation between times 0 and t at site i is related to the decorrelation of site j between the same times. The decrease of $g_4^{max}(r)$ (in figure 3) enables us to determine a cooperativity length above which the decorrelating events are not correlated (or not “cooperative”). We fit to the form $g_4^{max}(r) = \frac{g(\rho)}{r^{\alpha(\rho)}} \exp^{-r/\xi(\rho)}$. The fit works well enough: for ρ in the range 0.7–0.86 we find values of $\alpha(\rho)$ and $\xi(\rho)$ ranging from 0.22 to 0.64, and from 0.70 to 2.75 respectively. Again the cooperativity length $\xi(\rho)$ is very well fitted by a double exponential form: $\xi(\rho) \simeq 0.34 \exp(\exp 0.16/(1-\rho))$. We have determined a time scale and a cooperativity scale $\xi(\rho)$ that diverge as $\rho \rightarrow 1$. Note that the behaviour of $g_4^{max}(r)$ is more reminiscent of a strong glass of the type of the 3d Fredrickson-Andersen model, than of a fragile glass (see [24]), although the KA model is also fragile, but with a conserved order parameter.

Connected clusters of frozen particles. – In exploring length and time scales of KA we have also focused on the analysis of the connected clusters of blocked particles: we reconstruct the clusters of nearest-neighbor particles that have not moved at t from their initial position. We have analyzed them by computing their number and the probability distribution of clusters of size n , $P(n, t)$. We show in figure 4.a the number of such blocked clusters, that turns out to

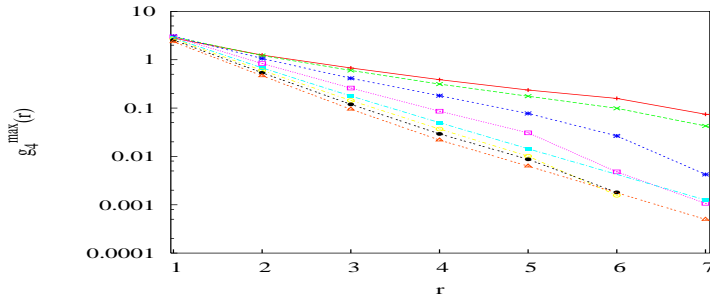


Fig. 3 – $g_4^{max}(r)$ as a function of the distance r . From top to bottom, $\rho = 0.86, 0.85, 0.83, 0.8, 0.77, 0.75, 0.73, 0.7$.

be maximum at a time $t_{cluster}$. We plot with different lines data at different density values. This time scale, close to τ_{trap} and t_{relax} , has again a behavior compatible with [10].

At small times the probability $P(n, t)$ is mainly composed of two distinct populations: large blocked clusters that dominate the rate of relaxation and small blocked clusters. As time passes some particles move, and the large initial blocked clusters decrease in size, giving rise to smaller clusters. At an intermediate timescale (which is very close to $t_{cluster}$) the two populations of blocked clusters merge. We show in figure 4.b $P(n, t_{cluster})$ for different density values. Here the behavior looks as a power law ($\sim \frac{1}{n^\mu}$, where $\mu \sim 1.3$) and one can observe a collapse of the curves for all densities; the origin of this unique exponent is unclear to us. At very long times the system relaxes completely: the persistent clusters only consist of a few particles, that will eventually fly. For $t \sim t_{cluster}$ the initial structure of clusters has been destroyed on small and large length scales: at this stage spatial cooperativity is maximum, and one can see that the particles not only move from the borders of blocked clusters, but also propagate inside, breaking big clusters into smaller ones of significantly different sizes.

We have studied the moments $\lambda(\rho) = \langle \lambda \rangle_{P^*}$ and $\sigma(\rho) = \sqrt{\langle \lambda^2 \rangle_{P^*} - \langle \lambda \rangle_{P^*}^2}$, where $\lambda \equiv n^{1/3}$, n is the cluster size and expectation values are taken over the probability distribution P^* at $t_{cluster}$. $\lambda(\rho)$ is the typical size of the blocked clusters that slow down the dynamics, and can hence be seen as a (maybe rough) determination of the length $\Xi(\rho)$, defined in [10] as the spacing between mobile regions. A fit actually gives $\lambda(\rho) \simeq 0.83 \exp(\exp(0.12/(1 - \rho)))$. The fluctuations measured by $\sigma(\rho)$ obey the same exponential law in ρ , but reach higher values than $\lambda(\rho)$.

Conclusions. – We have shown that dynamical geometrical constraints in the KA model are able to induce spatial correlations through different characteristic length scales, that all diverge in the same way as $\rho \rightarrow 1$. We show in figure 5 the behaviour of $\xi(\rho)$, $l_c(\rho)$, and $\lambda(\rho)$. They can be rescaled by a constant, and are shown together with the fit $y \sim \exp(\exp 0.16/(1 - \rho))$.

We have already noticed that also time scales (that grow in our allowed range far more than length scales, giving a far better way of discriminating between different behaviors) suggest a scaling law compatible with a double-exponential singularity at $\rho = 1$. We show in particular in figure 6 the time t^* defined from the maximum of $\chi(t)$ versus ρ : the fit with a double-exponential is surely preferred over the best fit to a power divergence at $\rho_c = 0.881$ (note that the y scale is logarithmic, and the power fit is far from the data).

In our study, $l_c(\rho)$ measures the correlation between sites of the persistence times. The coherence length $\xi(\rho)$ deduced from measurements of four-point correlation functions is the

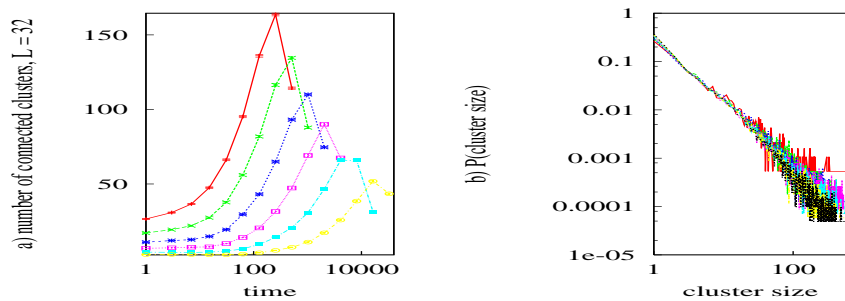


Fig. 4 – For ρ going from 0.7 to 0.8: a) number of persistent connected clusters (lower densities on the left, higher densities on the right); b) probability distribution of the number of particles in persistent clusters at $t_{cluster}(\rho)$ for all densities: one can observe the collapse of the curves.

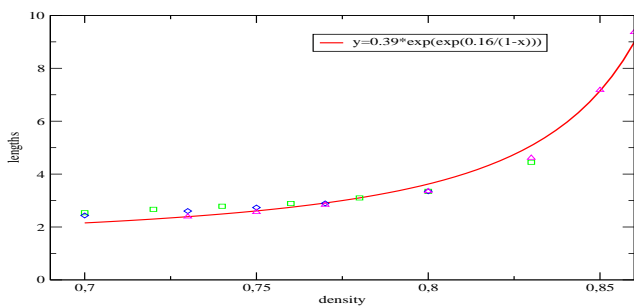


Fig. 5 – The three lengths, $\lambda(\rho)$ (squares), $1.78l_c(\rho)$ (diamonds), and $3.41\xi(\rho)$ (triangles) versus ρ , together with the best double-exponential fit.

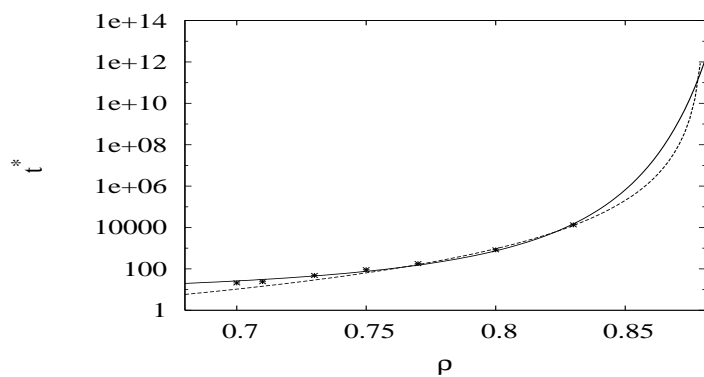


Fig. 6 – t^* versus ρ . The continuous line is for the best fit for a double-exponential singularity at $\rho = 1$, the dashed line is for the best power fit (with $\rho_c = 0.881$).

typical length of cooperative events for a given density. The typical length between mobile particles that contribute to the relaxation of the system $\Xi(\rho)$ can be estimated via $\lambda(\rho)$, the average size of persistent clusters up to $t_{cluster}$, the time of maximum cooperativity. Moreover, the spatial structure contains even more complexity, since the distribution of this length obeys a power-law, which still remains to be understood. An analytical solution of the KA model is lacking, and would give a more precise understanding of the relaxation laws, the persistence properties, the existence of a dynamical exponent z , and the distributions of cluster sizes, probably to be linked with an analogy with percolation problems [6, 10, 11].

Finally, we want to stress that the coherence length $\xi(\rho)$ is a priori independent of any growing length-scale that is believed to exist in a system without time-translational invariance dynamics (aging). In the version of the KA model studied here, there is no aging due to the flat energy landscape. However, an aging version would be able to show how $\xi(\rho, t_w)$ evolves with the age t_w . In particular it would be very interesting to study its behavior and that of $t^*(\rho, t_w)$ in this case and compare it to experimental data in aging jammed systems [23].

This work has been supported by EEC contracts HPRN-CT-2002-00307 (DYGLAGE-MEM) and HPRN-CT-2002-00319 (STIPCO), and by the ESF SPHINX network. EP thanks UMR 5825 (Montpellier) where this work was initiated, and the Physics Department at *La Sapienza*. We thank L. Berthier, J-P. Bouchaud, S. Franz, C. Godrèche, R. Monasson, V. Van Kerrebroeck and especially G. Biroli, W. Kob and C. Toninelli for discussions.

REFERENCES

- [1] F. Ritort and P. Sollich, *Adv. in Phys.* **52**, 219 (2003).
- [2] L. F. Cugliandolo, in *Slow Relaxations and Non-Equilibrium Dynamics in Condensed Matter*, edited by J.-L. Barrat et al. (Springer, Berlin 2003).
- [3] S. Whitlam and J. P. Garrahan, *J. Phys. Chem. B* **108**, 6611 (2004).
- [4] S. Butler and P. Harrowell, *J. Chem. Phys.* **95**, 4454 (1991); P. Harrowell. *Phys. Rev. E* **48**, 4359 (1993).
- [5] M.D. Ediger, *Annu. Rev. Phys. Chem.* **51**, 99 (2000).
- [6] W. Kob and H. C. Andersen, *Phys. Rev. E* **48**, 4364 (1993).
- [7] J. Kurchan, L. Peliti and M. Sellitto, *Europhys. Lett.* **39**, 365 (1997).
- [8] L. Berthier and J. P. Garrahan, *J. Chem. Phys.* **119**, 4367 (2003); L. Berthier and J. P. Garrahan, *Phys. Rev. E* **68**, 041201 (2003).
- [9] C. Toninelli, PhD Thesis, Università di Roma *La Sapienza*, October 2003, unpublished.
- [10] C. Toninelli, G. Biroli and D. Fisher, *Phys. Rev. Lett.* **92**, 185504 (2004); C. Toninelli and G. Biroli, cond-mat/0402314.
- [11] J. Adler, *Physica A* **171** (1991) 435.
- [12] S. Franz and G. Parisi, *J. Phys C* **12**, 6335 (2000).
- [13] C. Donati, S. Franz, G. Parisi and S. Glotzer, *J. Non-Cryst. Sol.* **307**, 215 (2002).
- [14] N. Lacevic, F. Starr, T. Schroeder, S. Glotzer, *J. Chem. Phys.* **119**, 7372 (2003); L. Berthier, *Phys. Rev. Lett.* **91** 055701 (2003).
- [15] S. Franz, R. Mulet and G. Parisi, *Phys. Rev. E* **65**, 021506 (2002).
- [16] J. P. Garrahan and D. Chandler, *Phys. Rev. Lett.* **89**, 035704 (2002).
- [17] B. Doliwa and A. Heuer, *Phys. Rev. E* **67**, 030501(R) (2003).
- [18] R. A. Denny, D. R. Reichman and J.-P. Bouchaud, *Phys. Rev. Lett.* **90**, 025503 (2003).
- [19] L. Berthier, *Phys. Rev. Lett.* **91**, 055701 (2003).
- [20] A. Buhot, J.P. Garrahan, *Phys. Rev. E.* **64**, 021505 (2001).
- [21] S. I. Simdyankin and N. Mousseau, *Phys. Rev. E* **68**, 041110 (2003).
- [22] H. Spohn, *Large Scale Dynamics of Interacting Particles* (Springer, Berlin 1991).
- [23] L. Cipelletti, H. Bissig, V. Trappe, P. Ballestat, S. Mazoyer, *J. Phys. C* **15** S257 (2003).
- [24] S. Whitlam et al., cond-mat/0408694. L. Berthier, J.P. Garrahan, cond-mat/0410076.